Isobaric analog resonances of the $N = 21$ nucleus ^{35}Si

N. Imai,[1,2,*] Y. Hirayama,[1] Y. X. Watanabe,[1] T. Teranishi,[3] T. Hashimoto,[4] S. Hayakawa,[4] Y. Ichikawa,[5] H. Ishiyama,[1] S. C. Jeong,[1] D. Kahl,[4] S. Kubono,[4] H. Miyatake,[1] H. Ueno,[5] H. Yamaguchi,[4] K. Yoneda,[5] and A. Yoshimi[5]

[1]*Institute of Particle and Nuclear Studies, High Energy Accelerator Research Organization (KEK), Oho 1-1, Tsukuba, Ibaraki 305-0801, Japan*

[2]*PH-Department, CERN, CH-1211 Geneva 23, Switzerland*

[3]*Department of Physics, Kyushu University, Fukuoka 812-8581, Japan*

[4]*Center for Nuclear Study, University of Tokyo, RIKEN Campus, 2-1 Hirosawa, Wako, Saitama 351-0198, Japan*

[5]*RIKEN Nishina Center, 2-1 Hirosawa, Wako, Saitama 351-0198, Japan*

(Received 16 December 2011; published 15 March 2012)

Neutron single-particle states in the neutron-rich nucleus ^{35}Si, which is located beside the $N = 20$ shell breaking nucleus ^{32}Mg, were investigated through their isobaric analog resonances. The excitation function for ^{34}Si+p elastic scattering was measured around 0° in the laboratory frame by the thick target inverse kinematics method with a ^{34}Si beam around 5 MeV/nucleon and a thick polyethylene target. Eight resonances were successfully observed. Angular momenta and proton and total widths of the resonances were assigned using R-matrix analysis. With the help of information of the β decay study, six isobaric analog resonances were identified. Spectroscopic factors and spin-parities of the corresponding parent states in ^{35}Si are presented.

DOI: 10.1103/PhysRevC.85.034313 PACS number(s): 21.10.Jx, 21.10.Hw, 25.40.Ny, 25.60.Bx

I. INTRODUCTION

Recent progress in nuclear structure modeling has been based on experimental foundations, and likewise experiments have been based on modeling. In particular, studies of the nuclear structure of radioactive nuclei, where protons and neutrons are combined with largely unbalanced ratios, are a challenge for current nuclear physics. Experimental studies have revealed exotic phenomena such as halo- [1] and neutron-decoupled nuclei [2] and magicity losses of neutron number $N = 20$ [3–6] not found in stable isotopes. To fully understand these phenomena, the nuclear structure in a wide range around these nuclei should be investigated.

Several experimental works have studied the nuclear structure around ^{32}Mg, and the results are consistently interpreted as showing that the magic number $N = 20$ disappears in this region. The first evidence of this was obtained by measuring the enhanced two-neutron separation energy of ^{31,32}Na [5]. A sudden decrease of the energy of the first 2^+ state from 3.33 to 0.88 MeV for ^{34}Si and ^{32}Mg [4,6], respectively, suggests that the onset of the deformation starts at ^{32}Mg, not at ^{34}Si. More direct evidence was obtained from comparing the enhanced quadrupole collectivities for ^{32}Mg [3] and ^{34}Si [7]. In the common picture explaining the shell breaking, there remain problems in the shell structure in this region. The experimental results for the spin-parity J^π of the ground state in ^{33}Mg obtained in various studies are inconsistent with each other [8–11].

In the framework of the shell model, the neutron pf orbitals are replaced with sd orbitals to reproduce the quadrupole nature in this region by introducing an enhanced tensor force and changing the single-particle energies accordingly [12]. The single-particle structures of the nuclei in this region will be a stringent test for the shell model Hamiltonian. Particularly for even more neutron-rich nuclei, the structure of ^{35}Si plays a vital role in determining the effective interaction, since this nucleus is considered to have pure single-particle states which define the location of the pf orbital [13].

In this article, we investigate neutron single-particle states in the $N = 21$ nucleus ^{35}Si through isobaric analog resonances (IARs) by means of proton resonance elastic scattering. Assuming an isospin symmetry of the nuclear force, neutron single-particle configurations in the nucleus ^{35}Si are identical to the configuration of protons in corresponding excited states appearing at high excitation energies in the isobaric nucleus ^{35}P, called isobaric analog states. When the analog state is above the proton separation energy S_p, the state is observed in the excitation function of elastic scattering on a target nucleus ^{34}Si as a resonance, called IAR. The resonance energy E_R, spectroscopic factor S, and angular momentum l can be deduced by R-matrix analysis [14,15] on the excitation function of differential cross sections at a given scattering angle.

When a parent state is close to a pure single-particle state, i.e., the state has a large S, a corresponding IAR would be observed as a significant resonance. Whereas, for a small S, typically $S \leqslant 0.1$, it is sometimes difficult to identify the IAR because there are often many lower isospin $T_<$ excitations comparable to the strength of $S \simeq 0.1$. In the case of an ideal IAR, almost all the total width $\Gamma_{\rm tot}$ is extinguished by proton width Γ_p due to the isospin conservation, which gives us a hint to identify the IAR. In addition, with help of other experimental studies, we can obtain more detailed spectroscopic information.

To date, four bound states have been observed in ^{35}Si from a measurement of β decay [6]. The g factor of the ground state was measured to be close to the Schmit value as a single-particle state of $7/2^-$ [16], which seems consistent with the doubly magic character of ^{34}Si. The ground state of

*nobuaki.imai@cern.ch

^{35}Si is located above ^{35}P by 10 500(40) keV [17]. The energy difference between the IAR and the corresponding parent state is determined by the Coulomb displacement energy Δ_c and the mass difference between a proton and neutron δ_{pn}. Using an empirical formula for Δ_c [18], each IAR is expected to be located above the parent state by $\Delta_c - \delta_{pn} = 4623$ keV. Since the S_p of ^{35}P is 12 190(14) keV, we would observe IARs in an excitation function of proton elastic scattering with a center-of-mass energy $E_{\mathrm{c.m.}}$ larger than 2933 keV.

II. EXPERIMENT

For unstable nuclei, proton resonance scattering with thick target inverse kinematics (TTIK) is useful [19] for obtaining the excitation function of proton elastic scattering. At 0° in the laboratory frame corresponding to 180° in the c.m. frame, the effect of potential scattering is smallest so that the feature of resonance scattering can be observed to be clearer. Due to the inverse kinematics, the energy of the recoil proton reaches four times higher than the c.m. energy $E_{\mathrm{c.m.}}$. Accordingly, the energy interval between the resonances in the c.m. energy is also projected to a laboratory-energy interval that is wider, and largest at 0° where it is four times wider. In addition, since the stopping power of protons is much smaller than that of the heavy incident ions, the elastic scattering excitation function may be measured over a wide range of energies with the use of a single fixed incident beam energy [20–27].

The experiment was performed at the accelerator facility operated by the RIKEN Nishina Center and Center for Nuclear Study, University of Tokyo. A secondary ^{34}Si beam was produced by projectile fragmentation of a 63-MeV/nucleon ^{40}Ar primary beam and was separated by the RIKEN projectile fragment separator (RIPS) [28]. Particle identification of the secondary beam was performed event-by-event by time-of-flight (TOF) between the timing signals measured by a plastic scintillator of 0.1 mm thickness located at the second focal plane of RIPS (F2) and the cyclotron rf signals. The momentum acceptance of RIPS was restricted to ±1% at the first focal plane in order to make a narrow timing distribution of the beam so that identification was enabled only with the TOF. After the particle identification, the energy of the beam ions was degraded to 4.4(12) MeV/nucleon at a secondary target with a 90 mg/cm^2 thick carbon plate placed just upstream of the plastic scintillator at F2. The effective thickness of the plate was tuned by tilting the angle with the respect to the beam axis. The incident energies of the beams upon the secondary target were determined by the timing difference between the plastic scintillator and two sets of parallel plate avalanche counters (PPACs) placed upstream of the target. The transmission between F2 and the final focal plane was as low as 34% due to multiple scattering in the carbon plate. The ^{34}Si beam had a typical intensity of 7×10^4 particles per second and a purity of 97% at the secondary target. The PPACs were also used to record the positions and angles of the projectiles incident upon the target.

The secondary target was a 10.9(5) mg/cm^2 thick polyethylene film. A 13.9(4) mg/cm^2 thick carbon film was also used to evaluate the number of protons produced by fusion evaporation

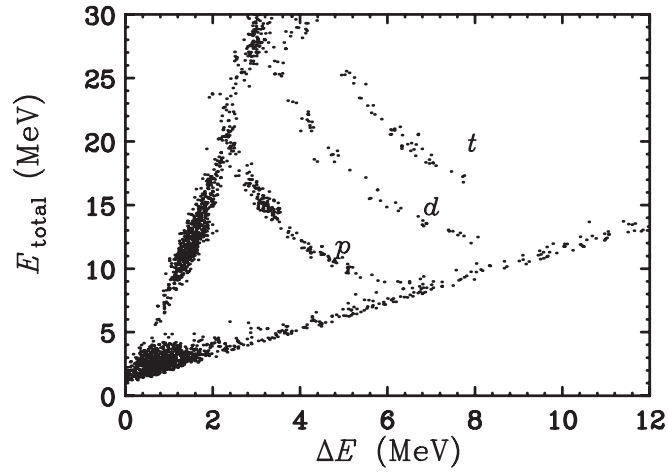

FIG. 1. Correlation between the energy deposit in the first SSD (ΔE) and the sum of those in the three SSDs (E_{tot}). Protons, deuterons, and tritons are indicated by p, d, and t beside the respective loci.

reactions. Although most of the beam ions stopped in the target, some of the ions, whose energies were higher than about 6.2 MeV/nucleon, punched through the target. Outgoing particles were measured by using three layers of silicon semiconductor detectors (SSDs) mounted at 0°. The distance between the SSDs and the target was 22 cm. The respective thicknesses were 0.5, 1.5, and 1.5 mm. Each sensitive area was 48 × 48 mm^2, which covered ±6.2° in the laboratory frame. The first-layer SSD had double-sided and orthogonally oriented 16 + 16 readout strips, allowing determination of the scattering angles of the particles. The particles were identified by the ΔE-E method. Figure 1 demonstrates the correlation between energy loss in the first SSD (ΔE) and the sum of energy losses in all the SSDs (E_{tot}). Protons were clearly separated from other particles. IARs will be observed above a proton energy E_p of about 12 MeV.

Energy calibration of the SSDs was performed in different runs with proton beams produced by the fragmentation reaction from ^{40}Ar. The energies of the protons were changed from 12 to 21 MeV by 1-MeV steps, restricting the rigidity of the protons with a narrow momentum slit of ±0.125%. The energies could be determined within 20 keV uncertainty.

The excitation functions of differential cross sections of protons observed at $\theta_{\mathrm{lab}} < 10.0°$ with the polyethylene and carbon targets are compared in Fig. 2(a). The cross section at each energy bin was deduced by taking into account the target thickness where the beam lost energy equal to the bin width and the energy distribution of the beam ions. $E_{\mathrm{c.m.}}$ was deduced from the measured proton energy and the scattering angle on an event-by-event basis by assuming the kinematics of elastic scattering and by considering the energy losses of both the incident heavy ions and the outgoing proton in the target. The energy loss was estimated using the SRIM-2008 code [29]. The energy resolution in E_{lab} was estimated to be 130 keV (σ), which was mainly derived from the detector energy resolution of 120 keV and the energy spread of 50 keV due to the angular uncertainty of 0.5°. By subtracting the carbon contribution from the cross sections measured with the

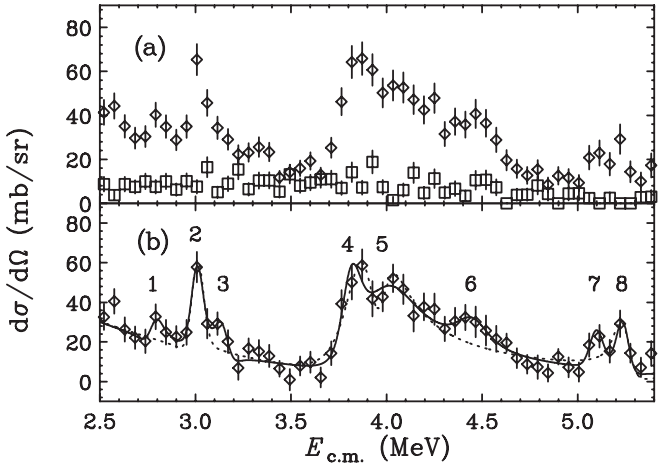

FIG. 2. Excitation functions of the proton elastic scattering. (a) Cross sections at $\theta_{lab} < 10.0^{\circ}$, measured with the polyethylene target with one day accumulation (diamond) and the carbon target with a half day accumulation (square). (b) Excitation function after subtracting the carbon contribution. The solid line denotes the best fit R-matrix calculation assuming eight resonances. The dotted line shows the result assuming four resonances. See the text for details.

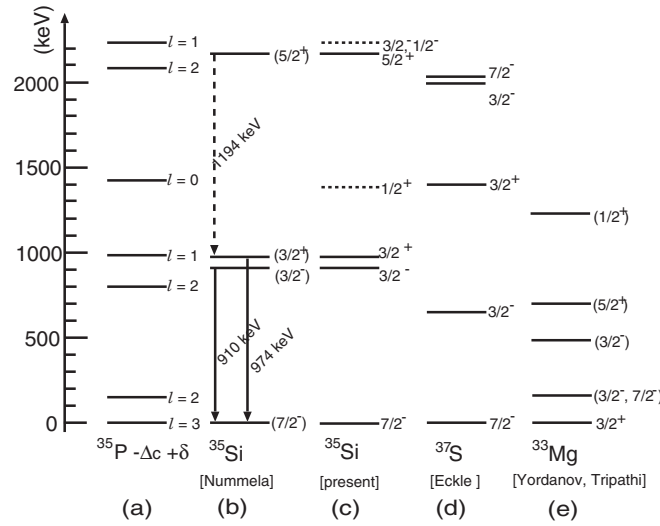

FIG. 3. Nuclear structure information of $N = 21$ nuclei from (a) proton resonance elastic scattering on ^{34}Si, (b) β decay of ^{35}Al (Nummela [6]), (c) a proposed level scheme of ^{35}Si. The candidates of new levels are presented by dotted lines. The level schemes of ^{37}S (Eckle [32]) and ^{33}Mg (Yordanov [9], Tripathi [10]) are shown for comparison in (d) and (e), respectively.

polyethylene target, the excitation function of the proton elastic scattering was obtained as presented in Fig. 2(b). Several resonances were clearly observed in the excitation function. Here, the error bars were derived from only the statistical uncertainties. Whereas the systematic error was estimated to be 12%, originating from the uncertainties of the solid angle (7%) and the effective target thickness (10%).

III. *R*-MATRIX ANALYSIS

An R-matrix calculation was performed to deduce E_R, l, Γ_p, and Γ_{tot} of the resonances. Assuming the values for l, a minimum value of χ^2 (χ^2_{min}) was searched for by changing the resonance parameters E_R, Γ_p, and Γ_{tot}, using MINUIT [30] with a condition of $\Gamma_{tot}/\Gamma_p \geqslant 1.0$. The R-matrix curve was obtained as the sum of the single resonances and folded with the experimental resolution. In the calculation, the potential scattering was obtained using the global optical model potential set [31]. For the all resonances, $j = l + 1/2$ was assumed for simplification. The resonance shape depends on the l value not on j. In the case of $j = l - 1/2$, the Γ_p value increases by $(2l + 1)/2l$.

First, we tried to fit the calculation to the experimental data with four resonances. The respective values for l were taken from the value of the corresponding parent states in ^{35}Si [6] as presented in Fig. 3(b). The initial E_R parameters were 2933, 3843, 3907, and 5101 keV estimated from the excitation energies of the parent states. The resultant excitation function demonstrated by the dotted line in Fig. 2(b) failed to reproduce the data, indicating that more resonances were required in the fit. At $E_{c.m.} \simeq 3$ MeV, we observed two other resonances on either side of the significant peak at 3 MeV. Around 4 MeV, there seems to be a broad peak which may consist of more than three resonances. Around 5 MeV, we observed two peaks.

We searched for χ^2_{min} by varying l of these eight resonances including the four whose parent states were previously discovered. The best fit curve was obtained by assuming $l = 0, 3, 2, 2, 1, 0, 2, 1$, respectively, from the lowest energy. The resultant curve is presented in Fig. 2(b), illustrating good agreement with the data. Here, $\chi^2_{min} = 24.1$ was obtained with 32 degrees of freedom. All the resonance parameters obtained are listed in Table I. Taking into account the g-factor measurement of ^{35}Si, the second resonance should be the lowest IAR. Indeed, the E_R is almost identical to the expected value of 2933 keV. Accordingly, the first resonance at 2783 keV can be regarded as a $T_<$ excitation. E^{pp}_{ex} in Table I represents the energy difference between the respective E_R and that of the second resonance. E^{pp}_{ex} and l of the resonances are compared with the excitation energies and J^{π} of the bound states in ^{35}Si in Fig. 3.

The spectroscopic factor S can be deduced from Γ_p using the formula [15]

$$S = \left. \frac{(N - Z + 1)2\mu r \Gamma_p}{2P^0_c e^{-2\delta^{l_{ij}}} \hbar^2 u^2_n(r)} \right|_{r=a_c}, \qquad (1)$$

where N and Z are the numbers of neutrons and protons, respectively, in the target nucleus, μ is the reduced mass of the proton, P^0_c is the optical penetrability, $a_c = 1.25(\sqrt[3]{34} + 1)$ is the matching radius, and $u_n(r)$ is the single-particle wave function of a bound state neutron in the parent state of (l, j) assuming a Woods-Saxon potential with radius and diffuseness parameters of 1.25 and 0.65 fm, respectively. $\delta^{l_{ij}}$ represents the imaginary part of the optical phase shift. The $u_n(r)$ was obtained by solving the Schrödinger equation to reproduce the neutron binding energy of the parent state. If the corresponding parent state was not discovered, the binding energy was estimated from the E^{pp}_{ex}. The obtained S are also tabulated in Table I. The listed uncertainties denote only the statistical

TABLE I. Parameters of eight resonances obtained by R-matrix analysis.

No.	l	E_R (keV)	$E_{\rm ex}^{pp}$ (keV)	Γ_p (keV)	$\Gamma_{\rm tot}$ (keV)	$\Gamma_{\rm tot}/\Gamma_p$	S	Type of excitation
1	0	2783(24)	−223(24)	4.6(28)	4.6(81)	1.0 (16)		$T_<$
2	3	3006(2)	0.0	1.6(4)	1.6(28)	1.0 (17)	0.63(16)	$T_>$
3	2	3151(24)	145(24)	3.3(27)	10.4(200)	3.2 (56)	0.19(15)	$T_<$
4	2	3809(18)	803(18)	26.7(69)	84.0(250)	3.1 (5)	0.79(20)	$T_>$
5	1	3990(36)	984(36)	185(43)	354(87)	1.9 (1)	1.37(32)	$T_>$
6	0	4450(44)	1444(44)	58.4(370)	215(150)	3.7 (11)	0.45(28)	$T_>$
7	2	5099(12)	2093(12)	3.8(9)	3.8(78)	1.0 (20)	0.04(1)	$T_>$
8	1	5200(15)	2194(15)	20.9(120)	32.0(220)	1.5 (0.6)	0.12(7)	$T_>$

ones. The systematic errors were estimated to be 13%, which mainly come from that of the cross sections. The systematics of S for the bound states at the low-lying states in $N = 21$ nuclei, which were obtained by (d,p) reactions [32–34], suggest that the f or p states have $S = 0.5 \sim 0.8$, whereas the s or d states, which are considered to be hole states have $S \simeq 0.05$.

IV. IDENTIFICATION OF IAR

A. Resonances around $E_R = 3$ MeV

As aforementioned, the second resonance can be identified as an IAR of the ground state of ^{35}Si from the assigned l and the E_R which is close to expectation. In addition, $S = 0.63(16)$ is in good agreement with the systematics as a single-particle state of $7/2^-$, supporting that the resonance is the IAR of an $l = 3$ state.

We assigned the third resonance as a $T_<$ excitation, although the strength is relatively large. If there is a low-lying parent state of $l = 2$ in ^{35}Si, a γ transition to the ground state should be observed in the β decay from ^{35}Al, but such a corresponding line was not reported [6].

B. Resonances around $E_R = 4$ MeV

By taking into account the l and the E_R, the fourth and fifth resonances can be assigned as the IARs of the parent states at 974 and 910 keV, respectively. The $3/2^-$ state in ^{35}Si was assigned from the systematics of the $N = 21$ nuclei [6]. The present experiment confirms the assignment. Although the order of the resonances was inverted, the respective Coulomb displacement energies deduced are 5307 and 5552 keV for the fourth and fifth resonances, which are within a typical deviation of ±150 keV [18] from the value of 5405 keV deduced from the empirical formula. As followed the assignment of the β decay study, when $J^\pi = 3/2^+$ is assumed for the $l = 2$ state, the obtained Γ_p and $\Gamma_{\rm tot}$ change to 41.0 (108) keV and 86.5(265) keV, respectively. S increases accordingly to 1.21(32). The S values are much larger than expected values of $S \simeq 0.05$ and 0.5, respectively, from the systematics. These large S values may be attributed to unresolved resonances around $E_{\rm c.m.} \simeq 4$ MeV. Thus, the resonance parameters of these resonances would be modified by further measurements with higher statistics and better energy resolution.

For the sixth resonance of $l = 0$, although the $\Gamma_{\rm tot} \gg \Gamma_p$, the resonance width is larger than the typical $T_<$ excitation of $S < 0.1$, suggesting that the state would be an IAR. If the resonance is an IAR, the corresponding parent state should be placed around $E_{\rm ex}^{pp} = 1440$ keV in the ^{35}Si. Unfortunately, the parent state could not be observed in the β decay from ^{35}Al, since the $E2$ transition of $5/2^+ \rightarrow 1/2^+$ should be hindered compared to the $M1$ transition of $5/2^+ \rightarrow 3/2^+$.

C. Resonances around $E_R = 5$ MeV

As expected from the β decay study, the seventh resonance can be considered as the IAR of the excited state at 2168 keV. The deduced S of the resonance is also consistent with the systematics of $l = 2$.

For the eighth resonance, the $\Gamma_{\rm tot} \simeq \Gamma_p$, suggesting the state is an IAR whose parent state was not observed yet. The parent state should be located around $E_{\rm ex}^{pp} = 2194$ keV in ^{35}Si. The systematics of J^π for the second $l = 1$ state in $N = 21$ nuclei suggests $J^\pi = 3/2^-$ of this parent state. Although the present S value of 0.12(7) is close to the $S = 0.17$ of the second $3/2^-$ in ^{41}Ca [34], the corresponding values for ^{39}Ar [33] and ^{37}S [32] are 0.08, 0.03, respectively, which do not show any systematic trend. In the case of $J^\pi = 1/2^-$, Γ_p and $\Gamma_{\rm tot}$ change to 58.0(160) and 58.0(180) keV, respectively. The S increases accordingly to 0.33(23), which is also close to the $S = 0.49$ of the $1/2^-$ state in ^{37}S. Since the systematic trend is not reliable for the second $l = 1$ state, we just assign an l value for the parent state.

V. DISCUSSION

A level scheme for ^{35}Si, proposed by taking into account the β decay study and the present results, is compared with those of ^{33}Mg and ^{37}S in Fig. 3(c). The assignment performed with the β decay was supported by the present experiment. In addition, the candidates of two new excited states were observed as shown by the dotted lines. Their energies are assumed to be the same as $E_{\rm ex}^{pp}$ in the figure.

The excitation energies and the order of J^π of the excited states in ^{35}Si resemble those of ^{37}S rather than that of ^{33}Mg, clearly indicating that this nucleus is located outside the "island of inversion." However, we can see the hint of the evolution of the $N = 20$ gap in the energy decrease of the first $d_{3/2}$ state at ^{35}Si, which is consistent with the shell model calculations [12,13].

Although the $1/2^+$ state in ^{37}S was not measured, by extrapolating the excitation energies of the $1/2^+$ states of ^{41}Ca and ^{39}Ar, the $1/2^+$ state can be expected to be around 1700 keV

in ^{35}Si. The present value of $E_{\rm ex}^{pp} = 1440$ keV is lower than the expectation, which appears to support a sudden jump in the evolution of the $s_{1/2}$ orbital at ^{35}Si [12].

The variation of S for the second $l = 1$ state in $N = 21$ nuclei remains an open question. A comparison with the theoretical spectroscopic factors of these states in ^{35}Si is anticipated for further understanding the shell evolution of this region.

VI. CONCLUSION

We observed eight resonances in the highly excited states in ^{35}P by measuring the proton resonance elastic scattering with ^{34}Si of about 5 MeV/nucleon employing the TTIK method to study the single-particle structure of ^{35}Si. Through the R-matrix analysis, we determined resonance parameters l, E_R, Γ_p, and $\Gamma_{\rm tot}$ of the resonances. By comparing the result of β decay, we confirmed the J^π of four bound states which were already observed. In addition, we assigned two candidates of the new states. We also deduced the S from the respective Γ_p value. Comparing theoretical S values should be helpful to understanding the shell evolution in this region.

Considering the simple experimental setup and large cross sections, the present work demonstrates that the proton resonance elastic scattering with TTIK method for IARs can be used as a powerful tool for studying neutron single-particle states in neutron-rich nuclei.

ACKNOWLEDGMENTS

We appreciate the RIKEN Nishina Center and CNS staff for their cooperation during the experiment. The present work was partly supported by a Grant-in-Aid for Scientific Research (20244036, 23244060) and Young Scientists (23740215) by the Japan Society for the Promotion of Science.

[1] I. Tanihata, H. Hamagaki, O. Hashimoto, Y. Shida, N. Yoshikawa, K. Sugimoto, O. Yamakawa, T. Kobayashi, and N. Takahashi, Phys. Rev. Lett. **55**, 2676 (1985).
[2] H. J. Ong *et al.*, Phys. Rev. C **78**, 014308 (2008); Z. Elekes, N. Aoi, Zs. Dombrádi, Zs. Fülöp, T. Motobayashi, and H. Sakurai, *ibid.* **78**, 027301 (2008).
[3] T. Motobayashi *et al.*, Phys. Lett. B **346**, 9 (1995).
[4] C. Détraz, D. Guillemaud, G. Huber, R. Klapisch, M. Langevin, F. Naulin, C. Thibault, L. C. Carraz, and F. Touchard, Phys. Rev. C **19**, 164 (1979).
[5] C. Thibault, R. Klapisch, C. Rigaud, A. M. Poskanzer, R. Prieels, L. Lessard, and W. Reisdori, Phys. Rev. C **12**, 644 (1975).
[6] S. Nummela *et al.*, Phys. Rev. C **63**, 044316 (2001).
[7] R. W. Ibbotson *et al.*, Phys. Rev. Lett. **80**, 2081 (1998).
[8] S. Nummela *et al.*, Phys. Rev. C **64**, 054313 (2001).
[9] D. T. Yordanov, M. Kowalska, K. Blaum, M. De Rydt, K. T. Flanagan, P. Lievens, R. Neugart, G. Neyens, and H. H. Stroke, Phys. Rev. Lett. **99**, 212501 (2007).
[10] V. Tripathi *et al.*, Phys. Rev. Lett. **101**, 142504 (2008).
[11] R. Kanungo *et al.*, Phys. Lett. B **685**, 253 (2010).
[12] T. Otsuka, T. Suzuki, M. Honma, Y. Utsuno, N. Tsunoda, K. Tsukiyama, and M. Hjorth-Jensen, Phys. Rev. Lett. **104**, 012501 (2010).
[13] F. Nowacki and A. Poves, Phys. Rev. C **79**, 014310 (2009).
[14] A. M. Lane and R. G. Thomas, Rev. Mod. Phys. **30**, 257 (1958).
[15] W. J. Thompson, J. L. Adams, and D. Robson, Phys. Rev. **173**, 975 (1968).
[16] G. Neyens *et al.*, Eur. Phys. J. Special Topics **150**, 149 (2007).
[17] P. M. Endt and R. B. Firestone, Nucl. Phys. A **633**, 1 (1998).
[18] J. Jänecke, in *Isospin in Nuclear Physics*, edited by D. H. Wilkinson (North-Holland, Amsterdam, 1969), p. 341, Eq. (8.107).
[19] K. P. Artemov, M. S. Golovkov, V. Z. Goldberg, V. V. Pankratov, A. E. Pakhomov, I. N. Serikov, and V. A. Timofeev, Sov. J. Nucl. Phys. **55**, 1460 (1992).
[20] R. Coszach *et al.*, Phys. Rev. C **50**, 1695 (1994).
[21] L. Axelsson *et al.*, Phys. Rev. C **54**, R1511 (1996).
[22] D. W. Bardayan *et al.*, Phys. Rev. Lett. **83**, 45 (1999).
[23] G. V. Rogachev *et al.*, Phys. Rev. C **64**, 061601 (2001).
[24] T. Teranishi *et al.*, Phys. Lett. B **556**, 27 (2003).
[25] C. Ruiz *et al.*, Phys. Rev. C **71**, 025802 (2005).
[26] G. V. Rogachev *et al.*, Phys. Rev. C **67**, 041603(R) (2003).
[27] N. Imai *et al.*, Eur. Phys. J. A **46**, 157 (2010).
[28] T. Kubo, M. Ishihara, N. Inabe, H. Kumagai, I. Tanihata, K. Yoshida, T. Nakamura, H. Okuno, S. Shimoura, and K. Asahi, Nucl. Instr. Meth. B **70**, 309 (1992).
[29] J. Ziegler, SRIM-2008 [http://www.srim.org/].
[30] CERN program library.
[31] F. D. Becchetti Jr. and G. W. Greenless, Phys. Rev. **182**, 1190 (1969).
[32] G. Eckle, H. Kader, H. Clement, F. J. Eckle, F. Merz, R. Hertenberger, H. J. Maier, P. Schiemenz, and G. Graw, Nucl. Phys. A **491**, 205 (1989).
[33] S. Sen, C. L. Hollas, and C. W. Bjork, and P. J. Riley, Phys. Rev. C **5**, 1278 (1972).
[34] F. J. Eckle *et al.*, Nucl. Phys. A **506**, 159 (1990).